

Structural position of the Tolmachova active magmatic center in the south of Kamchatka and its origin

A.G. Nurmukhamedov*, M.D. Sidorov

Research Geotechnological Center of the Far Eastern Branch of the Russian Academy of Sciences, Petropavlovsk-Kamchatsky, Russian Federation

Abstract. The article is of a review nature, where the results of deep geological and geophysical studies carried out in the south of Kamchatka and in the nearest water area of the Pacific Ocean are presented. A description of the volumetric density model and its analysis in combination with other data are given. Information on the structural position of the Tolmachova active magmatic center (TAMC) and its origin is supplemented. As a result of the studies, a mantle protrusion was revealed, which has closed contours and was formed in the Nachikinskaya transverse dislocation zone no later than the Early Miocene. The sizes of the major and minor axes of the protrusion are ~ 123 and 84 km, respectively. In the lower part of the mantle protrusion, at a depth of 35–45 km, local areas of decompression are identified, which are associated with centers of melting. The formation of the protrusion may be caused by the pressure of ultrabasic magma from the upper mantle and its subsequent intrusion into the lower layers of the Earth's crust. The protrusion occurred along a weakened zone formed at the initial stage of shear dislocation that occurred in the Miocene-Pliocene time. Differentiation of magma entering the Earth's crust from melting centers, as well as heat flows from the same sources, form areas of focal melting and, as a consequence, lead to the formation of an intrusive massif of medium to medium acidic composition. Periodic movement of magma along a weakened zone in the TAMC area is accompanied by a swarm of weak earthquakes. The TAMC is genetically related to the mantle protrusion and is an integral part of it.

Inflection zones of the subducting oceanic lithosphere are areas of accumulation of tectonic stress and its periodic unloading in the form of earthquakes. The highest density of seismic events with magnitude $M \geq 5$ is observed in the seismic lineament located closest to the coastline – in the zone of maximum slab bending in the depth range of ~ 30–50 km.

Keywords: upper mantle, mantle protrusion, Earth's crust, subduction, terrane, density model, seismic lineament

Recommended citation: Nurmukhamedov A.G., Sidorov M.D. (2025). Structural position of the Tolmachova active magmatic center in the south of Kamchatka and its origin. *Georesursy = Georesources*, 27(3), pp. 139–150. <https://doi.org/10.18599/grs.2025.3.18>

Introduction

The deep structure of South Kamchatka (Fig. 1), where modern geodynamic processes occur, is of considerable interest to a wide range of specialists involved in the forecasting of mineral resources, earthquakes and volcanic eruptions.

The area is characterized by active volcanism and high seismicity; there are a large number of natural

hydrothermal vents, several gold deposits and epithermal ore occurrences have been discovered (Fig. 2). The Porozhistoye deposit and a number of gold ore occurrences to the east of it form the Karymshinsky ore cluster, which is part of the Tolmachova active magmatic center (TAMC) zone (Nurmukhamedov, 2017; Nurmukhamedov et al., 2020). Active hydrothermal activity is observed in the TAMC zone. Thus, on the flanks of the paleovolcano with the center of Sopka Goryachaya (Fig. 3) there are magmatic sources of hydrothermal activity, including ones located the north of the Sopka – the Bolshe-Bannoe steam-water mixture geothermal field. In the Neopleistocene-Holocene time in the south of Kamchatka areal volcanism was

*Corresponding author: Alexander G. Nurmukhamedov
e-mail: nurmuxamedov1949@mail.ru

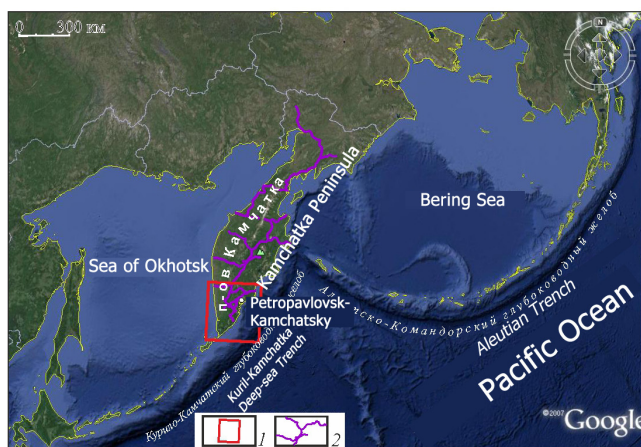


Fig. 1. 1 – contours of the study area; 2 – regional geophysical profiles

activated, represented on the day surface by groups of low (100–300 m) cinder cones of predominantly basaltic composition (Vazheevskaya, 1980). The latest manifestation of this volcanism (Holocene) was noted in the TAMC area, in the interfluvium of the Tolmachova and Karymchina rivers (Fig. 2, 3), where geodynamic processes continue to the present day. Thus, in 1987–1988 a swarm of weak ($M \leq 5$) earthquakes was recorded (Fig. 3). The maximum density of epicenters is concentrated in a local area called the Tolmachova epicentral zone (TEZ) (Nurmukhamedov, 2017). The depth of the hypocenters was about 8 km, which is close to the depth to the roof of the Tolmachova intrusive massif of medium to medium acidic composition (Nurmukhamedov et al., 2020).

The earthquake swarm coincides with the area of the highest concentration of cinder cones. Seismic activity is explained by the movement of magma along a weakened zone – an eruptive crack of sublatitudinal strike (Nurmukhamedov et al., 2020; Nurmukhamedov, Sidorov, 2019a). Earthquakes are of the volcanotectonic type, which are not associated with volcanic eruptions (Chubarova, 2006). The TAMC was first discovered by electrical exploration studies using the magnetotelluric sounding (MTS) method in 1979–1981 on the Ust-Bolsheretsk Settlement – Shipunsky Peninsula profile (Fig. 3). A contrasting crust-mantle anomaly of electrical conductance was revealed (Nurmukhamedov, Smirnov, 1985), localized in the upper layers of the Earth's crust in the area of the Bolshe-Bannoye steam-water mixture geothermal field. Induction vectors showed that the effective epicenter of the anomaly is located to the south of the profile, where in the second half of the 1980s – early 1990s two additional mutually intersecting geophysical profiles were developed: Opala Mountain – Vakhil River and Apacha Village – Mutnaya Bay (Fig. 3) using the earthquake converted-wave method (ECWM) and magnetotelluric sounding (MTS). Along each profile, deep sections were constructed using the

ECWM (Nurmukhamedov et al., 2016), two-dimensional geoelectric (Moroz et al., 1995; Nurmukhamedov et al., 2020) and density (Nurmukhamedov et al., 2020; Nurmukhamedov, Sidorov, 2019b) models were calculated, covering the Earth's crust and the upper mantle. The modeling results showed that the electrical conductance anomaly is located in the depth range from 8–10 to 30–35 km. In plan, the dimensions of the anomalous object are $\sim 50 \times 60$ km (Fig. 3). Based on a set of geophysical data, geological and geophysical models of the structure of the Earth's crust and the upper mantle were created (Nurmukhamedov et al., 2020; Nurmukhamedov, Sidorov, 2019b).

For a volumetric representation of the deep structure of the study area, density models were calculated and sections were constructed along additional profiles linking the ECWM-MTS profiles. Methods for constructing vertical two-dimensional (2D) density model for a network of profiles and their volumetric representation are presented in a special article (Sidorov, Nurmukhamedov, 2022), the method for constructing a volumetric density model of South Kamchatka is presented in the article (Nurmukhamedov, Sidorov, 2022). Using computer technologies, the resulting model can be viewed from any angle, obtain vertical density sections in the selected direction and make horizontal sections at any depth. The model provides for several levels in terms of coverage and detail. The first level is an overview level, with the size of the elementary cells that make up the model of $4 \times 4 \times 4$ km. This level covers the territory of Kamchatka from the latitude of the Ichinskaya Sopka and Tolbachinskaya Sopka volcanoes in the north to Cape Lopatka in the south, with the waters of the Sea of Okhotsk and the Pacific Ocean, including a fragment of the Kuril-Kamchatka deep-sea trench (Fig. 4). At the second level, in more detail, the TAMC area and its immediate flanks are characterized (Nurmukhamedov, Sidorov, 2022). The size of the cubic cells is $1 \times 1 \times 1$ km. Fig. 5 shows a volumetric model of the third research level with cell sizes of $0.5 \times 0.5 \times 0.5$ km (Sidorov, Nurmukhamedov, 2022). This part of the model directly covers the TAMC area (see the contours of the site in Fig. 3). A block saturated with mafic and ultramafic intrusions is highlighted in the Earth's crust by an equal density surface of 2.85 g/cm^3 . A detailed description of the block and its flanks is given in the article (Nurmukhamedov, Sidorov, 2022). Here we will only note that the high-density object ($\geq 2.85 \text{ g/cm}^3$) is located in the zone of the mantle protrusion, which will be characterized below.

To the southeast of the TAMC there is the Pribrezhny Horst, which is a fragment of the terrane of the same name. The horst is marked by a positive gravity field (PGF) anomaly, a significant part of which is located in the Pacific Ocean (Fig. 3).

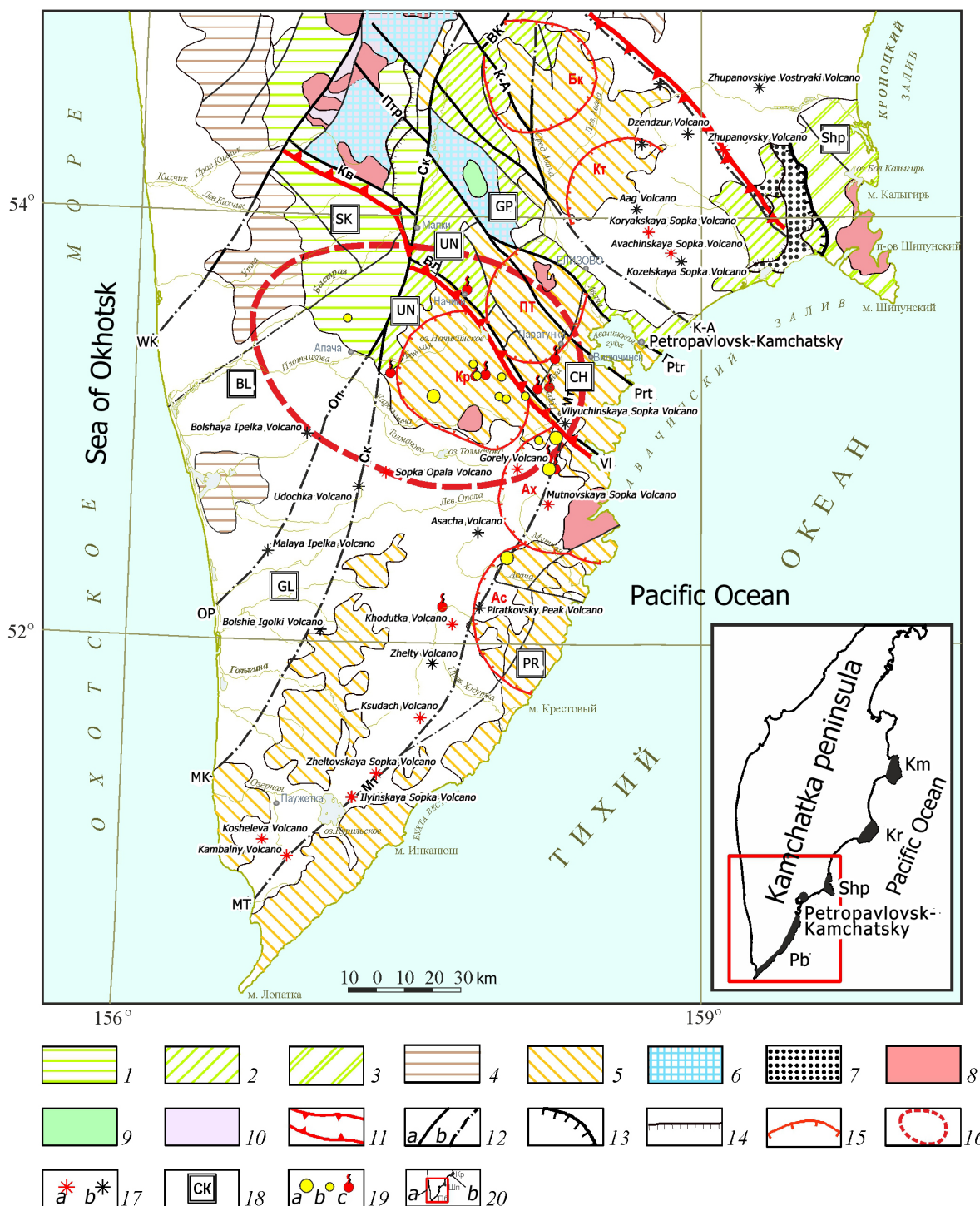


Fig. 2. Fragment of the Tectonic Scheme of the Koryak-Kamchatka Folded Region (Nurmukhamedov, 2013) – with simplification and additions. 1 – Koryak-West Kamchatka folded zone; 2 – East Kamchatka subzone of the Olyutor-East Kamchatka folded zone; 3 – Oceanic folded zone; 4 – West Kamchatka superimposed trough; 5 – Kuril-South Kamchatka island-arc volcanic zone; 6 – protrusions of the metamorphic basement of the Koryak-Kamchatka folded region; 7 – polymictic mélangé; intrusive formations: 8 – mainly of intermediate and siliceous composition of the Cretaceous, Paleogene, Neogene ages; 9 – the basic composition of the Cretaceous age; 10 – metamorphic and crystalline formations of the base of folded zones; 11 – boundaries of the Nachikinskaya transverse dislocation zone (Nachikinskaya TDZ); 12 – main faults outcropping on the daylight surface (a), overlapped by overlying formations (b). NE directions: WK – West Kamchatka, MK – Middle Kamchatka, EK – East Kamchatka, Op – Opalinsky, Mt – Mutnovsky; NW directions: K-A – Krutogorsko-Avachinsky, Ptr – Petropavlovsky, Prt – Paratunsky, Kv – Kvinumsky, VI – Vilyuchinsky; 13 – Vatynsky thrust; 14 – secondary thrusts; 15 – boundaries of volcano-tectonic structures (VTSs): Bk – Bakeningskaya, Kt – Kitkhoyskaya, PT – Plotnikovskaya, Kr – Karymshinskaya, Akh – Akhomtenskaya, As – Asachinskaya; 16 – contours of the mantle protrusion; 17 – active volcanoes (a), extinct (b); 18 – names of structures and their designations: SK – Sredinno-Kamchatsky horst-anticlinorium, BL – Bolsheretskoye uplift, GL – Golyginskaya depression, UN – Unkanovichsky horst, GP – Ganalsko-Petropavlovsky horst, PR – Pribrezhny Horst; 19 – gold deposits (a) and ore occurrences (b), sources and deposits of thermo-mineral waters (c); 20 – contours of the study area (a), terranes and their names (b): Km – Kamchatka, Kr – Kronotsky, Shp – Shipunsky, Pb – Pribrezhny (Coastal).

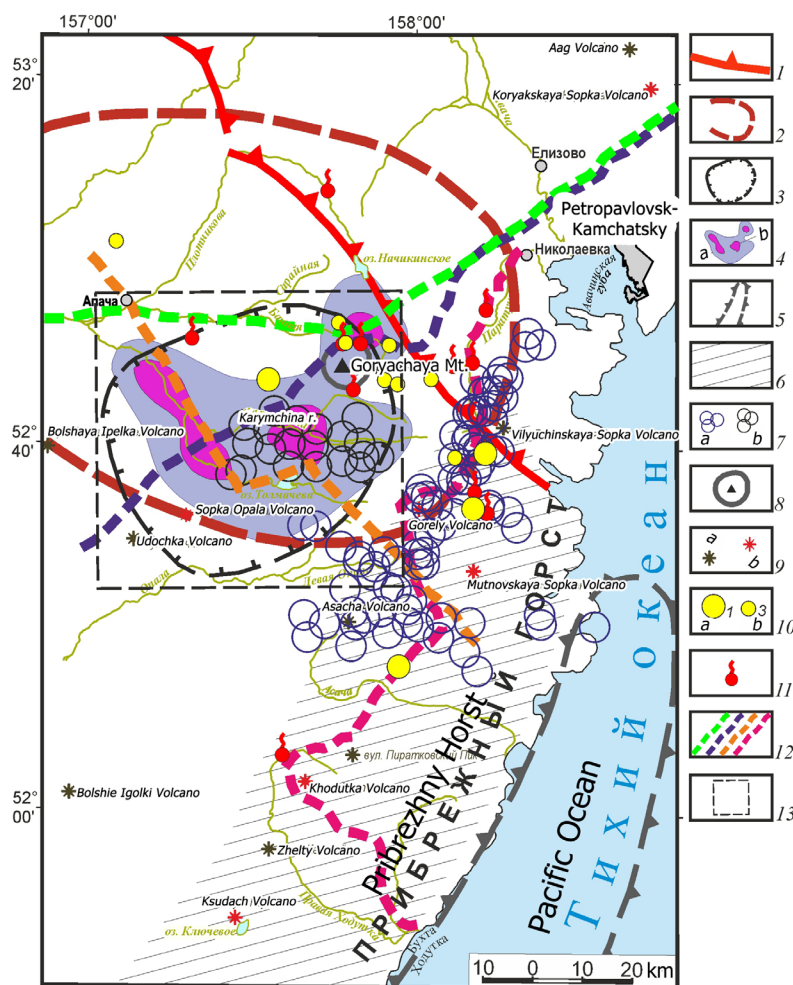


Fig. 3. Map of local earthquake epicenters recorded from 1981 to 1988 (based on materials from (Nurmukhamedov, Sidorov, 2023) with simplification and additions). 1 – southwestern boundary of the Nachikinskaya TDZ; 2 – contours of the mantle protrusion; 3 – boundary of the crust-mantle conductance anomaly formed in the zone of the Tolmachevo active magmatic center (TAMC); 4 – contours of the decompaction zone at a depth of ~ 40 km (a), areas of maximum decompaction in the depth interval of 35–45 km (b) – proposed melting centers; 5 – gravity maximum; 6 – zone of high-gradient gravity field – the area of modern active volcanism; 7 – epicenters of earthquakes (h = 0 ÷ 40 km) recorded during the time periods of 1981–1985 (a) and 1987–1988 (b); 8 – contours of the Sopka Goryachaya paleovolcano; 9 – extinct (a) and active (b) volcanoes; 10 – deposits (a) and ore occurrences (b) of the gold-silver formation; 11 – hydrothermal springs and fields; 12 – geophysical profiles: colored in green – the Ust-Bolsheretsk Village – Shipunsky Peninsula profile (MTS – 1979–82), blue – the Opala Mountain – Vakhil River profile (ECWM-MTS – 1989–1992), orange – the Apacha Village – Mutnaya Bay profile (ECWM-MTS – 1987–1989), purple – the Khodutka Bay – Nikolaevka Village profile (ECWM-MTS – 2009–2010); 13 – boundaries of the 3D density model with elementary cell sizes of 0.5×0.5×0.5 km.

The western boundary of the horst is expressed in the form of a gravity step, extended in the north-northeast direction. A seismic lineament (Nurmukhamedov, Sidorov, 2023) with a length of ~ 70 km (Fig. 3) was recorded along this zone. The lineament is located in the zone of recent extensions – in a rift zone 30–40 km wide, formed in the area of the maximum bend of the paleosubduction slab. The structure began to form in the Oligocene. Active and extinct volcanoes are located in the zone. In conclusion, it should be noted that this article is of a review nature and is intended to supplement the information on the structural position of the TAMC and its origin. The article describes the volumetric density

model (Nurmukhamedov, Sidorov, 2022; Sidorov, Nurmukhamedov, 2022) and its analysis in combination with other data. The entire study area is covered by gravimetric, aeromagnetic, geological surveys at a scale of 1:200,000, and in the southeast of Kamchatka, work was carried out to study the local range of earthquake epicenters (Nurmukhamedov, Sidorov, 2023). All the data accumulated over the past decades indicate that the TAMC is a unique object (Nurmukhamedov et al., 2020; Nurmukhamedov, Sidorov, 2022; Nurmukhamedov, Sidorov, 2023), requiring close attention from volcanologists, seismologists, hydrogeologists and specialists in the field of ore geology.

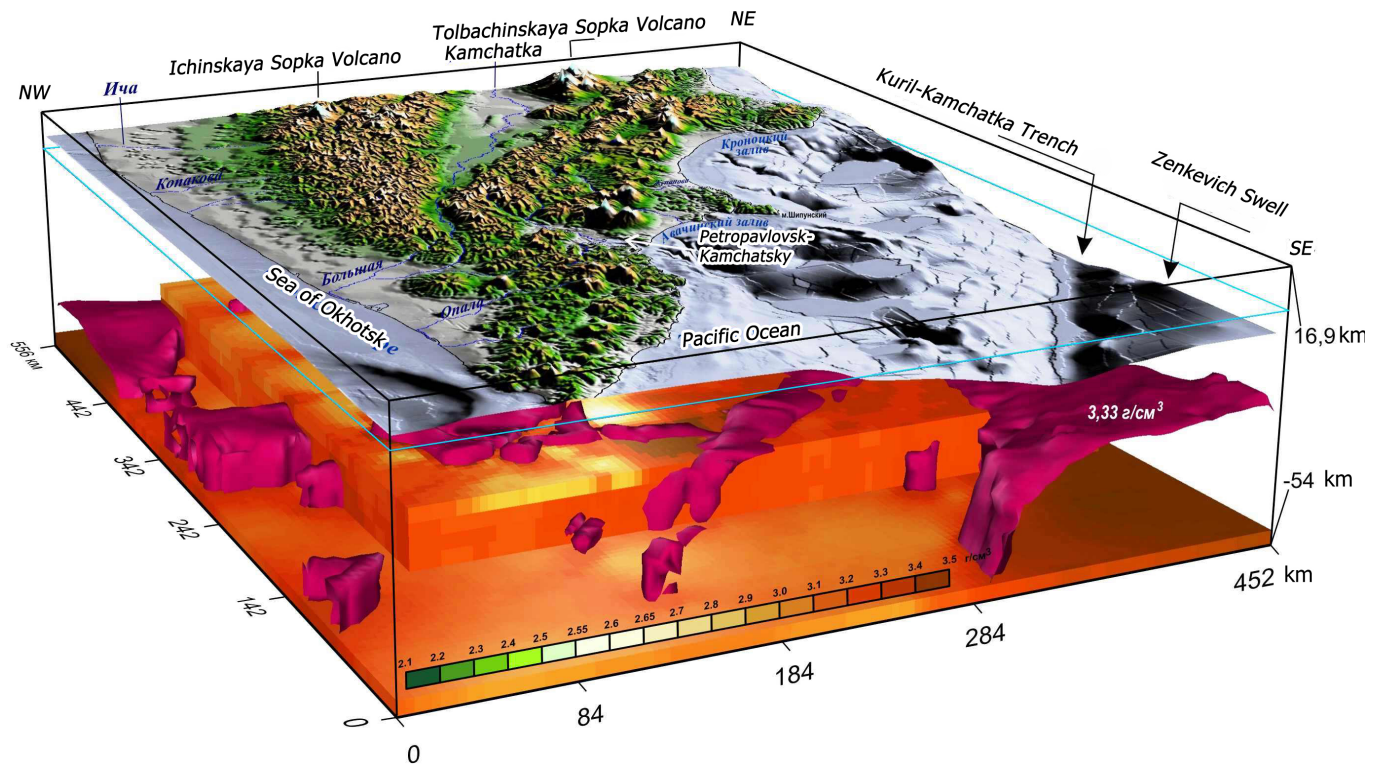


Fig. 4. Block diagram of the overview density model of the Earth’s crust and upper mantle of South Kamchatka (Nurmukhamedov, Sidorov, 2022). In the block diagram, the vertical scale is increased by two times; some cells are “turned off”; the relief is “raised” by 3 km; the true sea level is shown by the blue line; the equal density surface of the layer with a density of 3.33 g/cm³ is shown in purple.

Density modeling results

The description of the volumetric model and its geological interpretation are presented in the publication (Nurmukhamedov, Sidorov, 2022). In this article, we will briefly note only those results that reflect the deep structure of southern Kamchatka and the nearest ocean area. Fig. 4 shows an overview model, which highlights isodensity surfaces identified with the boundaries of high-density layers and blocks (≥ 3.33 g/cm³). Such density is characteristic of upper mantle rocks – peridotites. The model shows two surfaces plunging to great depths in the west-northwest direction. The equal density surface under the Pacific Ocean is interpreted as a fragment of the top of the modern subduction slab. The surface fragment recorded under the peninsula is identified with the top of paleosubduction. The latter was blocked due to the attachment of the island arc block to paleo-Kamchatka at the end of the Eocene – beginning of the Oligocene (Nurmukhamedov, Sidorov, 2023; Seliverstov, 2009). In the southeastern part of the model, the steeply inclined equal density surface is the boundary of the upper mantle block of high density (3.36 g/cm³), presumably represented by rocks with a high garnet content (Nurmukhamedov, Sidorov, 2022).

Fig. 6B shows a density section of the overview model (Fig. 4) along the S4 line (Fig. 6A) (Nurmukhamedov, Sidorov, 2022), and below its geological interpretation is presented. Fig. 6C shows a diagram of the interaction

of the continental lithosphere with the subducting oceanic one.

Analysis of the geological and geophysical model along the S4 line and discussion of the results

In the northwestern part of the model (60–190 km of the line), a clearly defined structure more than 120 km long is observed, limited by the protrusions of the Moho boundary and the overlying layers of the Earth’s crust. The amplitude of the protrusion in different places ranges from several kilometers to 10 km or more. In the southeastern half of the model, a fragment of paleosubduction (subduction up to and including the Eocene) and a fragment of modern subduction with an extension zone in the area of maximum bending are distinguished (Nurmukhamedov, Sidorov, 2022). Note the gentle, and in places step-like, immersion of the top of the oceanic lithosphere.

Figure 7 shows the epicenters of earthquakes with a magnitude of $M \geq 3.5$ in the depth range of 0–30 and 30–50 km for the period of instrumental observations from 1962 to 2013 (Nurmukhamedov, 2013).

The data are taken from the earthquake catalog (<http://www.emsd.ru/ts/>).

Most of the epicenters are located to the east of the coast of Kamchatka in the ocean area in the form of three extended strips – seismic lineaments parallel to

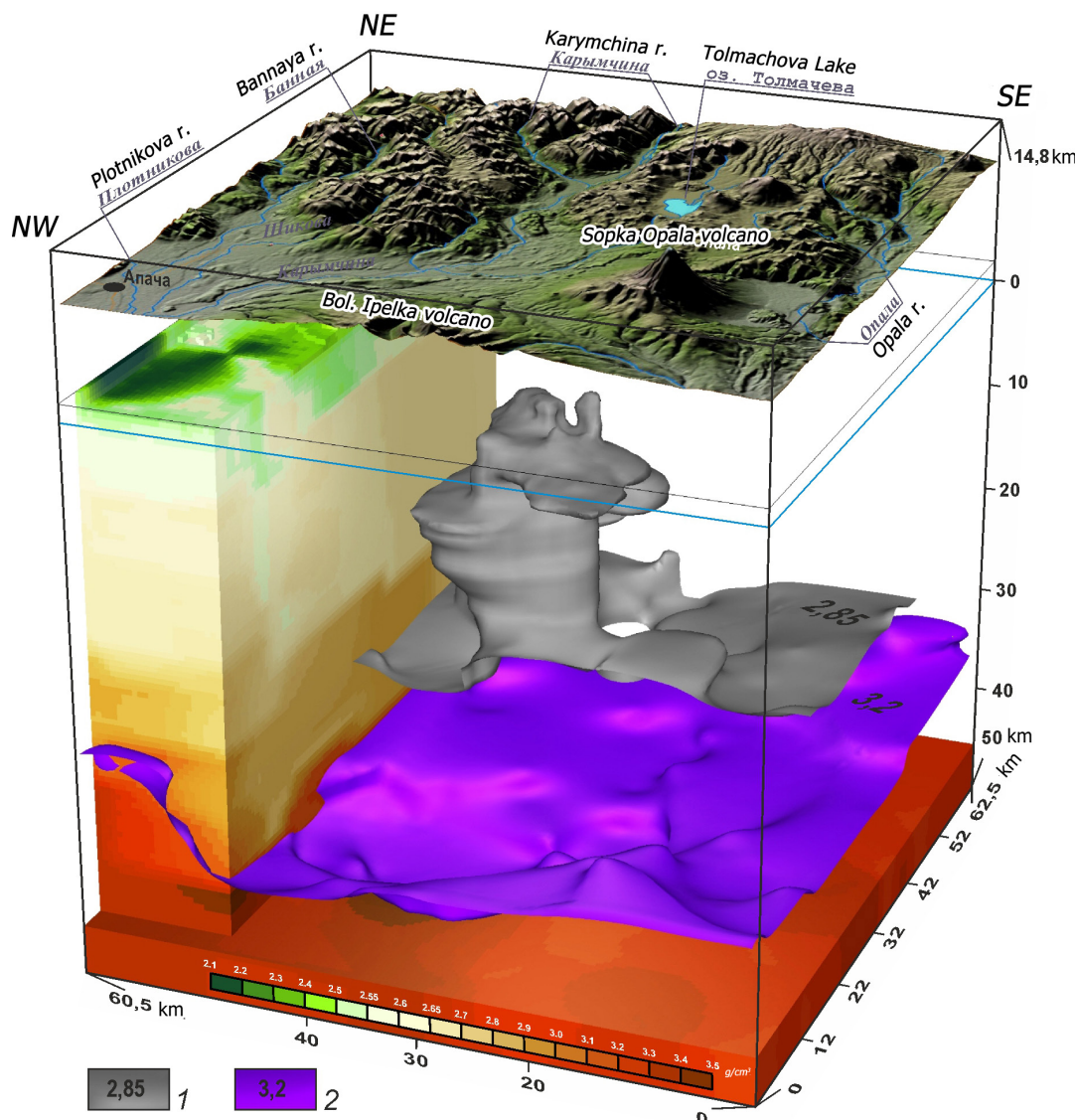


Fig. 5. Block diagram of the density model of the Earth's crust in the southern part of the Kamchatka Peninsula (Sidorov, Nurmukhamedov, 2022). View from the southwest (for the contours of the area, see Fig. 3). The size of the elementary 3D cell is $0.5 \times 0.5 \times 0.5$ km. The vertical scale of the Earth's surface relief is increased by two times, some cells in the model are "turned off". The relief is raised by 10 km, the true sea level is shown by the blue line. 1–2 – morphology of equal density surfaces of layers with a density of 2.85 g/cm^3 (1) and 3.2 g/cm^3 (2).

the eastern coast of the peninsula. In each lineament, a line can be drawn that will mark the central (axial) part of the seismically active region. Comparison of seismic data with the geological and geophysical model (Fig. 6) indicates the coincidence of the zone of maximum bending of the modern subduction slab (280–310 km of the line) with the axial part of the seismic lineament located closest to the coastline. Probably, the formation of tectonic stress and its release in the form of earthquakes occur in the process of advancing the oceanic lithosphere through the zone of maximum bending at a depth of 30–50 km, where the formation of the extension zone occurs. This assumption is confirmed (Nurmukhamedov, 2013) in the distribution of earthquake epicenters by the depth intervals of hypocenters (Fig. 8). The highest density of seismic events with a magnitude of $M \geq 5$ is

observed actually in the depth interval of 30–50 km.

The seismic lineament that is the next farthest from the coastline coincides with the reverse bend section (350–360 km). And finally, the third lineament that is the farthest from the coast coincides with the bend in the area of the uppermost step of the top of the modern subduction (400–420 km). Probably, tectonic stresses with their subsequent unloading in the form of seismic events are also formed in these two bends.

In the central part of the geological and geophysical model (150–250 km), the area of interaction of the marginal (overhanging) part of the continental lithosphere and oceanic paleosubduction is distinguished. Geological and geophysical studies (Nurmukhamedov, Sidorov, 2022; Nurmukhamedov, Sidorov, 2023) show that in the Oligocene (according to I.D. Petrenko

(1999) no later than the middle Miocene), in the zone of maximum bend of the “torn off slab”, the formation of a rift zone began, in which volcanic activity occurred in the Oligocene-Quaternary time. A large number of active and extinct volcanoes of Southeast Kamchatka are located in the extended rift zone. At the boundary of lithospheric plates of various types, magmatic chambers

are located (Fig. 6), identified according to MTS data (Nurmukhamedov, Sidorov, 2023) and confirmed by density modeling (Nurmukhamedov, Sidorov, 2022). The model shows that one of the chambers is located in the feeding area of the Mutnovskaya Sopka volcano. Subduction blocking occurred as a result of accumulation of critical mass in the accretion zone.

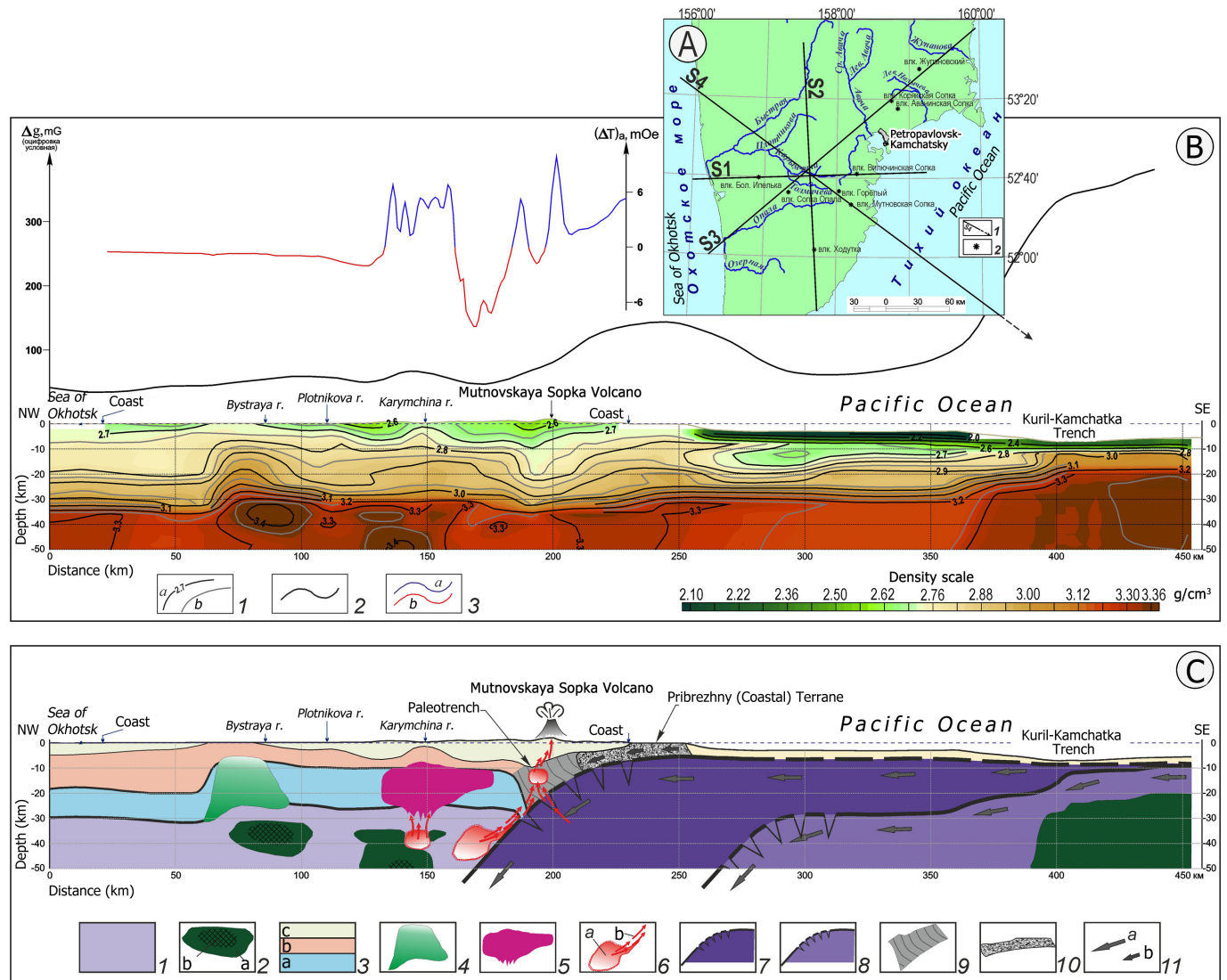


Fig. 6. Density section (B) of the volumetric model (Fig. 4) (Nurmukhamedov, Sidorov, 2022) and schematic geological and geophysical model (B) of the interaction of lithospheric plates along the S4 line (A). Captions to Fig. 6A: 1 – lines of density sections and their numbers; 2 – volcanoes. Fig. 6B: 1 – main (a), intermediate (b) isodenses with density values measured in g/cm³ (section of main isodenses is 0.1 g/cm³, intermediate – 0.05 g/cm³); 2–3 graphs of geophysical anomalies: 2 – in the Bouguer reduction (conventional level), 3 – magnetic field (a – positive, b – negative). Fig. 6C: Continental (overhanging) lithospheric plate: 1 – upper mantle; 2 – zones of development of ultramafic rocks with abnormally high density (≥ 3.3 – 3.35 g/cm³) (a) and areas of peridotite eclogitization located in them (≥ 3.4 g/cm³) (b); 3 – layers of the Earth’s crust: granulite-basite (a), granite-metamorphic (b), Mesozoic-Cenozoic volcanogenic-sedimentary rock complex (c); 4 – a block of the Earth’s crust saturated with intrusions from ultramafic to mafic composition; 5 – intrusive massif of diorite-granodiorite composition (Nurmukhamedov et al., 2020; Nurmukhamedov, Sidorov, 2022); 6 – presumed melting centers identified on the basis of on MTS data (Nurmukhamedov, Sidorov, 2023) and confirmed by density modeling (Nurmukhamedov, Sidorov, 2022) (a), direction of movement of magmatic melts and heat flows (b); 7 – fragment of paleosubduction (subduction up to and including the Eocene) with an extension zone in the area of maximum slab bending; 8 – fragment of modern subduction with an extension zone; 9 – accretion zone; 10 – Pribrezhny (Coastal) terrane; 11 – direction of movement of subductions (a) and island arc block (b) in the process of its attachment to the marginal part of the continental lithosphere.

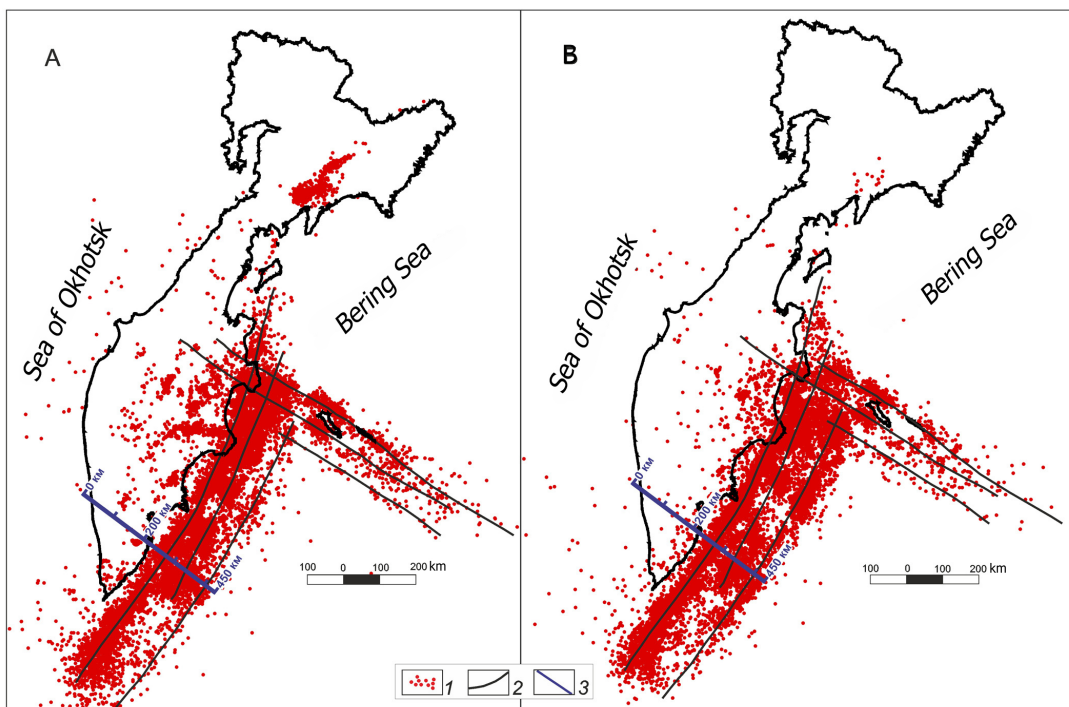


Fig. 7. Location of earthquake epicenters with focal depths of 0–30 km (A) and 30–50 km (B) ($M \geq 3.5$). 1 – earthquake epicenters; 2 – axes of high seismicity zones; 3 – line S4 of the density section and geological-geophysical model (see Fig. 6A).

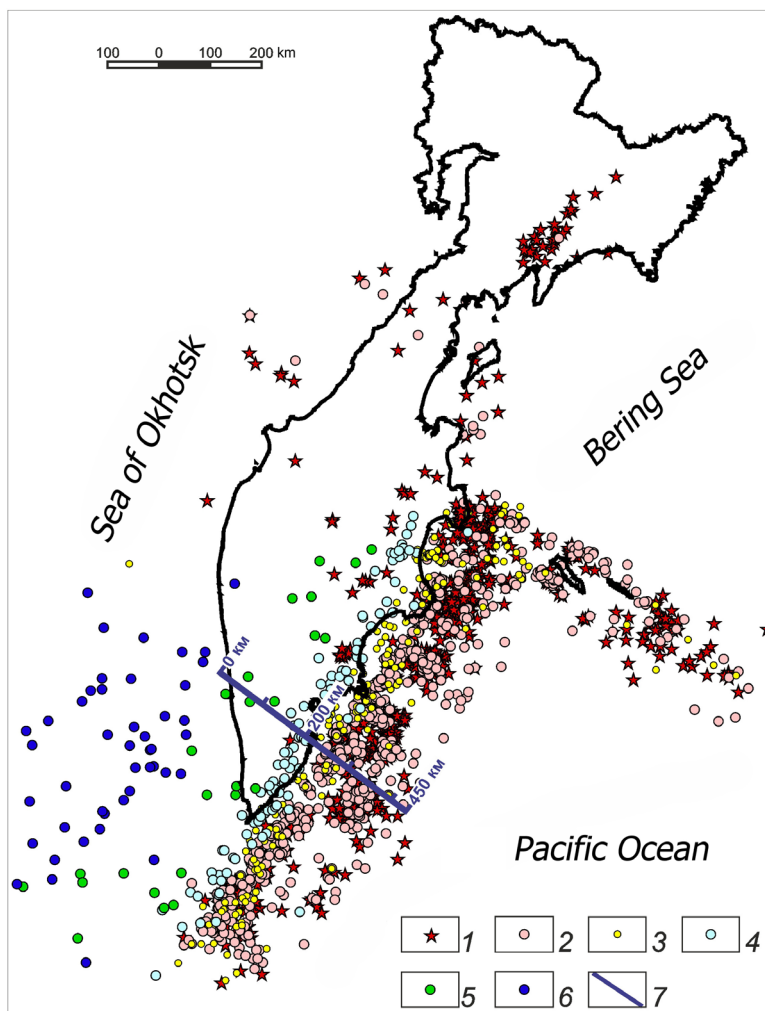


Fig. 8. Location of epicenters of earthquakes with magnitude $M \geq 5$ by hypocenter depth intervals. 1–5 – depth intervals (km): 1 – 0–30, 2 – 30–50, 3 – 50–100, 4 – 100–200, 5 – 200–400, 6 – 400–701; 7 – line S4 of the density section and geological-geophysical model (see Fig. 6A).

The blocking process was completed by the attachment of the Pribrezhny Terrane (Fig. 6C) to paleo-Kamchatka at the end of the Eocene – beginning of the Oligocene. According to some estimates (Nurmukhamedov, Sidorov, 2023), the Pribrezhny Terrane is the southern fragment of the Achaiwayam-Valagin Terrane.

In the upper part of the section there is a layer of Mesozoic-Cenozoic volcanogenic-sedimentary rock complex, in which there is a section (180–200 km) of maximum immersion of the base of the layer to a depth of up to 10 km. Probably, this depression is a fragment of an ancient deep-sea trench – a paleotrench.

Mantle protrusion. What could have caused the formation of the aforementioned high-amplitude protrusion of the Moho boundary? At first glance, the protrusion could have formed under the influence of lateral pressure of the subducting oceanic lithosphere under the marginal part of the continental lithosphere. But then the protrusion should be traced along the entire paleosubduction front for many hundreds of kilometers. Let us consider vertical sections of the volumetric density model in other places of the ocean-continent transition region (Fig. 9). Sections L1, L2 and L3 are located orthogonally to the coastline of Southeast Kamchatka parallel to line S4, which passes through the center of the TAMC (the location of the lines is shown in the diagram in Fig. 9).

Analysis of the density section farthest from TAMC along line L1 shows the absence of characteristic isodense bends of 3–3.3 g/cm³, which would reflect the protrusion of the Moho boundary and the overlying crustal layers. On the contrary, a rather smooth horizontally layered density distribution along the lateral is observed, with a smooth immersion of layers from the ocean side. In addition, the absence of a high-gradient transition from the Earth's crust to the upper mantle, typical of other areas of Kamchatka, is noted, which indicates the absence of a clearly defined boundary between these lithosphere layers in this place. Line L2 is located to the southwest of S4 at a distance of slightly more than 50 km. The section records two clearly defined crust-mantle decompression zones. One of them is located under the active Khodutka volcano, the second is on the line between the Udochka and Malaya Ipelka volcanoes (Fig. 2). Probably, the decompression is associated with the deep part of the feeding systems of volcanic structures. The characteristic extended protrusion of the Moho boundary and the lower crustal layers, as noted in the density section along the S4 lines (Fig. 6), is not observed. To the northeast of the S4 line, at a distance of about 70 km, there is a section along the L3 line. The section runs along the strike of the

Nachikinskaya TDZ (Fig. 2). The density distribution in terms of depth and lateral extent is quite complex, but, nevertheless, as in the previous section, the subsidence of the high-density layer (≥ 3.0 – 3.2 g/cm³) from the ocean side is confidently observed. In the center of the section there is a decompression area, which the authors explain by the presence of an accretion zone of ancient subduction (subduction up to and including the Eocene) in this place.

Thus, the table-shaped protrusion of the Moho boundary and the overlying crustal layers is absent both southwest and northeast of line S4. This protrusion is reliably visible only in sections along lines S1-S4 (Nurmukhamedov, Sidorov, 2022), which intersect in the center of the TAMC (Fig. 6A for the location of the lines). If we mark the boundaries of the protrusion on each line and smoothly connect them, we obtain an oval structure (Nurmukhamedov, Sidorov, 2024), elongated in the west-northwest direction (Figs. 2, 3). The length of the major and minor axes of the protrusion is ~ 123 and 84 km, respectively. Therefore, the identified structure is isometric and has closed contours.

A characteristic feature of the protrusion is the presence of high-density formations (≥ 3.4 g/cm³) in the pre-roof part of the upper mantle (Fig. 6), which, according to the authors (Nurmukhamedov, Sidorov, 2022), is associated with the eclogitization of peridotites. In addition, in the ledge zone (Fig. 6) and above it (Nurmukhamedov, Sidorov, 2022), it is assumed that there are blocks in the Earth's crust saturated with intrusions of ultrabasic and basic composition. It seems that the protrusion was formed as a result of squeezing ultrabasic magma from the upper mantle into the lower layers of the Earth's crust. And in this case, the term “mantle protrusion” should be quoted.

Among the high-density formations, at a depth of 35–45 km, localized areas of decompression are distinguished, identified by the authors with centers of melting. From the focal area, heat flows penetrate into the upper layers through weakened zones, forming areas of focal melting in the crust, as a result of which an intrusive massif of medium-medium acidic (diorite-granodiorite) composition was formed in the depth range from 8–10 to 30–35 km. The periodic movement of magma along the weakened zone is accompanied by a swarm of weak earthquakes. Long-term circulation of postmagmatic solutions mixed with meteoric waters leads to the formation of ore occurrences and gold deposits (Nurmukhamedov et al., 2020; Nurmukhamedov, Sidorov, 2022).

Structurally, the mantle protrusion adjoins the southwestern boundary of the Nachikinskaya TDZ (Fig. 2, 3) and partially overlaps it with its eastern flank.

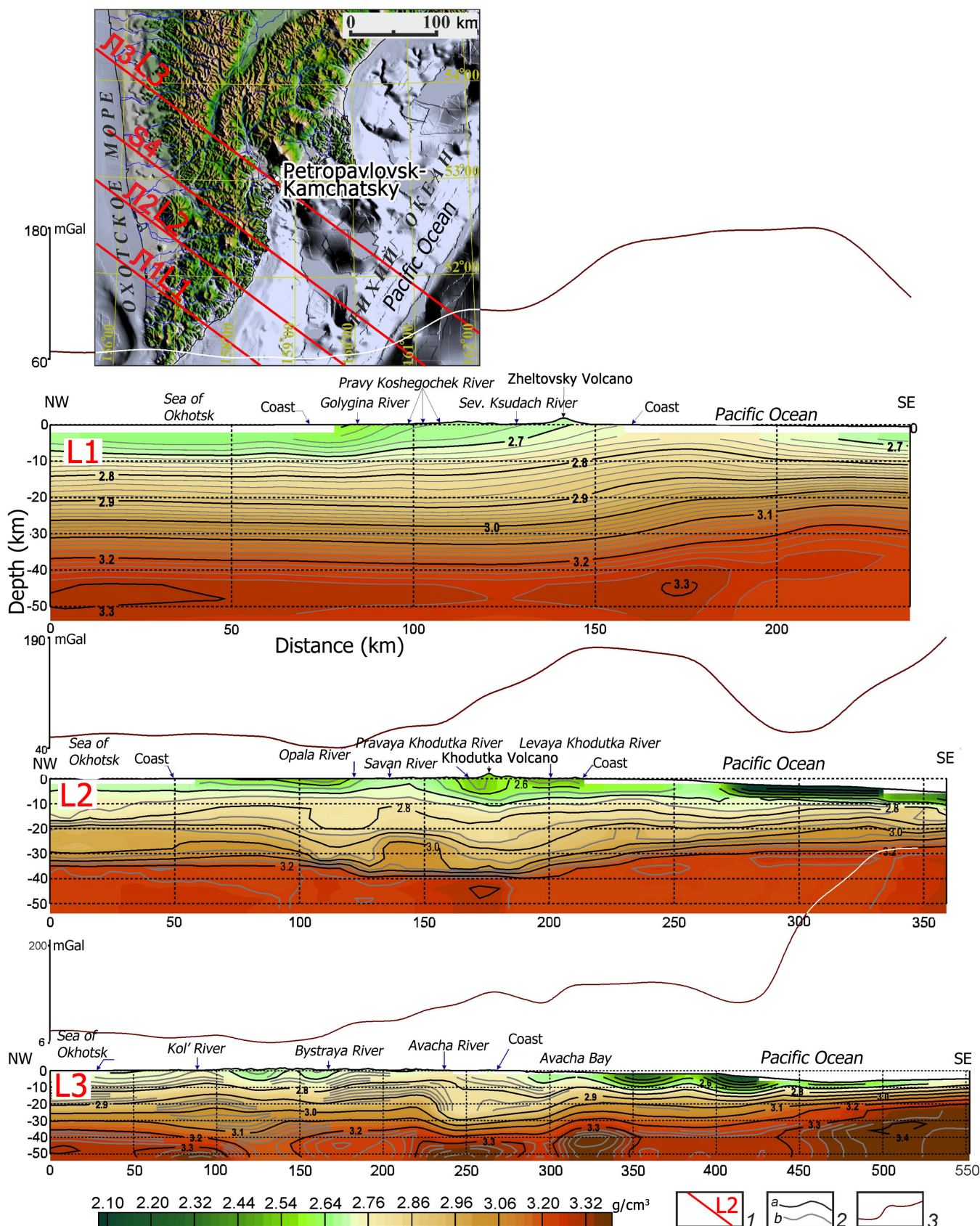


Fig. 9. Sections of the volumetric density model (Fig. 4) along lines L1, L2, L3. 1 – lines of density sections and their designations; 2 – main (a), intermediate (b) isodenses (intermediate isodenses are drawn through 0.02 g/cm³ on lines L1, L3 and through 0.05 g/cm³ on L2); 3 – Bouguer anomaly graph (conventional level).

However, if we pay attention to the shift in the lines along which the Asachinskaya and Akhomtenskaya volcano-tectonic structures (VTSs) are located on one side, and the Karymshinskaya, Plotnikovskaya, and Kitkhoiskaya on the other (Fig. 2), it is easy to see that the central part of the protrusion is still included in the zone of transverse dislocations with a left-lateral shift amplitude of about 50–60 km. According to M.M. Lebedev et al. (1979), the strike-slip dislocation occurred in the Miocene-Pliocene time. Subvolcanic formations and intrusions of diorite-granodiorite composition of Miocene age are developed in the protrusion zone (Geological Map..., 2005). The mantle protrusion is not disturbed by a transform fault, which indirectly indicates its formation after a shear dislocation. However, the intrusive massif of medium to medium acidic composition (Fig. 6) was formed after the introduction of ultrabasic rocks into the protrusion zone, i.e., after the formation of the mantle protrusion. The latter factor suggests that the protrusion was formed no later than the Early Miocene.

Conclusions

1. The Tolmachevo active magmatic center is genetically related to the mantle protrusion and is its integral part.

2. The mantle protrusion is not widespread along the paleosubduction front (subduction up to and including the Eocene). The protrusion structure has closed contours and was formed in the zone of transverse dislocations no later than the Early Miocene. The dimensions of the major and minor axes of the mantle protrusion are ~ 123 and 84 km, respectively. In the lower part of the protrusion, at a depth of 35–45 km, local areas of decompression are identified, identified with melting centers.

3. The formation of the mantle ledge may be caused by the pressure of ultrabasic magma from the upper mantle and its subsequent intrusion into the lower layers of the Earth's crust. The intrusion occurred along a weakened zone formed at the initial stage of the shear dislocation that occurred in the Miocene-Pliocene time.

4. The differentiation of magma entering the Earth's crust from melting centers, as well as heat flows from the same sources, form areas of focal melting and, as a consequence, lead to the formation of an intrusive massif of medium to medium acidic composition (Fig. 6C). The periodic movement of magma along the weakened zone is accompanied by a swarm of weak earthquakes (Nurmukhamedov et al., 2020; Nurmukhamedov, Sidorov, 2019a).

5. The inflection zones of the subducting oceanic lithosphere are areas of accumulation of tectonic stress and its periodic unloading in the form of earthquakes. The highest density of seismic events with magnitude

$M \geq 5$ is observed in the seismic lineament located closest to the coastline – in the zone of maximum slab bending in the depth range of ~ 30–50 km.

Acknowledgments

This work was supported by Research Geotechnological Center of the Far Eastern Branch of the Russian Academy of Sciences, State Assignment No. 075-01178-23-00, funded by the Ministry of Science and Higher Education of the Russian Federation.

The authors express their sincere gratitude to the reviewers for their valuable comments and suggestions, which contributed to the improvement of this work.

References

- Chubarova O.S. (2006). Volcanic Earthquakes. The Great Russian Encyclopedia. Moscow: Vol. 6, p. 91. (In Russ.)
- Geological Map and Map of Useful Fossils of Kamchatka Oblast and Koryak Autonomous Okrug (2005). Ed. A. F. Litvinov, B. A. Markovsky, V. P. Zaitsev. Scale 1:1 500000. St. Petersburg: VSECEL. (In Russ.)
- Lebedev M.M., Aprelkov S.E., Ezhov B.V., Kharchenko Yu.I. (1979). Island Arc Systems of the Koryak–Kamchatka Folded Region. *Vulkanologiya i seismologiya*, 5, pp. 30–36. (In Russ.)
- Moroz Yu.F., Nurmukhamedov A.G., Loshchinskaya G.A. (1995). Magnetotelluric sounding of the Earth's crust of Southern Kamchatka. *Vulkanologiya i seismologiya*, 4–5, pp. 127–138. (In Russ.)
- Nurmukhamedov A.G. (2013). Results of work on the project “Creation of a seismotectonic zoning scheme for the Koryak–Kamchatka folded region based on a summary of deep geological and geophysical works”. Report. Petropavlovsk-Kamchatsky: Kamchatgeologiya, 295 p. (In Russ.)
- Nurmukhamedov A.G. (2017). Bath and Karymshinskije hydrothermal systems – energy sources in the south of Kamchatka. *Mining informational and analytical bulletin*, 32, pp. 347–367. (In Russ.) <https://doi.org/10.25018/0236-1493-2017-12-32-347-367>
- Nurmukhamedov A.G., Sidorov M.D. (2019a). Tolmachevsky active magmatic center (South Kamchatka) and its heat–power capacity as estimated by deep geophysical surveys. *3rd International Geothermal Conference. IOP Conf. Series: Earth and Environmental Science* 367 012015. <https://doi.org/10.1088/1755-1315/367/1/012015>
- Nurmukhamedov A.G., Sidorov M.D. (2019b). Deep structure and geothermal potential along the regional profile set from Opala Mountain to Vakhil' River (Southern Kamchatka). *2nd International Geothermal Conference. IOP Conf. Series: Earth and Environmental Science* 249 012041. <https://doi.org/10.1088/1755-1315/249/1/012041>
- Nurmukhamedov A.G., Sidorov M.D., Moroz Yu.F. (2020). A model of the deep structure of the Earth's crust and upper mantle in the area of the Karymshinsky gold-ore cluster according to geophysical data (South Kamchatka). *Georesursy = Georesources*, 22(1), pp. 68–76. <https://doi.org/10.18599/grs.2020.1.63-72>
- Nurmukhamedov A.G., Sidorov M.D. (2022). Model of the structure of Southern Kamchatka based on the results of 3D density modeling and a set of geological and geophysical data. *Pacific Geology*, 41(2), pp. 25–43. (In Russ.) <https://doi.org/10.30911/02074028-2022-41-2-25-43>
- Nurmukhamedov A.G., Sidorov M.D. (2023). The structure of the lithosphere and its influence on the gold potential of Southeastern Kamchatka. *Vestnik KRAUNTS. Nauki o Zemle*, 59(3), pp. 20–41. (In Russ.) <https://doi.org/10.31431/1816-5524-2023-3-59-20-41>
- Nurmukhamedov A.G., Sidorov M.D. (2024). The Tolmachevsky active magmatic center in southeastern Kamchatka and its structural position. Volcanism and related processes. *Proc. XXVII Sci. Conf. Petropavlovsk-Kamchatskiy: IViS DVO RAN*, pp. 183–186. (In Russ.)
- Nurmukhamedov A.G., Smirnov V.S. (1985). Results of deep electromagnetic studies in Southern Kamchatka. Geology and useful minerals of the Koryak–Kamchatka folded region. Proc. V Kamchatka Geological Conf. Eds.: Pozdeev A.I., Kharchenko Yu.I., Yarotsky G.P., Lebedev M.M. Petropavlovsk-Kamchatsky: Kamchatka Regional Organization Scientific and Technical Association-Mining, pp. 69–82. (In Russ.)
- Nurmukhamedov A.G., Nedyadko V.V., Rakitov V.A., Lipatyev M.S. (2016). Lithosphere boundaries in Kamchatka based on earthquake converted wave data. *Vestnik KRAUNTS. Nauki o Zemle*, 29(1), pp. 35–52. (In Russ.)

Petrenko I.D. (1999). Gold-silver formation of Kamchatka. St. Petersburg: VSEGEI, 116 p. (In Russ.)

Seliverstov N.I. (2009). Geodynamics of the junction zone of the Kuril-Kamchatka and Aleutian island arcs. Petropavlovsk-Kamchatsky: KamSU Publishing House, 191 p. (In Russ.)

Sidorov M.D., Nurmukhamedov A.G. (2022). Three-Dimensional Image of Crustal Density Model: A Case Study in South Kamchatka. *Russ. Geol. Geophys.*, 63(10), pp. 1189–1206. <https://doi.org/10.2113/RGG20204328>

Vazheevskaya A.A. (1980). Areal Volcanism. Long-Lived Center of Endogenous Activity of Southern Kamchatka: Collective Monograph. Ed. Yu. P. Masurenko. Moscow: Nauka, pp. 39–41. (In Russ.)

Manuscript received 20 November 2024;

Accepted 28 February 2025;

Published 20 September 2025

© 2025 The Authors. This article is published in open access under the terms and conditions of the Creative Commons Attribution (CC BY) License (<https://creativecommons.org/licenses/by/4.0/>)

About the Authors

Alexander G. Nurmukhamedov – Cand. Sci. (Geology and Mineralogy), Leading Researcher. Research Geotechnological Center of the Far Eastern Branch of the Russian Academy of Sciences

P.O. Box 56, Severo-Vostochnoye shosse, 30, Petropavlovsk-Kamchatsky, 683002, Russian Federation
e-mail: nurmuxamedov1949@mail.ru

Mikhail D. Sidorov – Cand. Sci. (Geology and Mineralogy), Leading Researcher. Research Geotechnological Center of the Far Eastern Branch of the Russian Academy of Sciences

P.O. Box 56, Severo-Vostochnoye shosse, 30, Petropavlovsk-Kamchatsky, 683002, Russian Federation
e-mail: smd1952z@gmail.com